HADRON COLLIDERS VERSUS e^+e^- COLLIDERS

(a contribution to the round table from the BCF group)

M. Basile, G. Bonvicini, G. Cara Romeo, L. Cifarelli, A. Contin,
M. Curatolo, G. D'Ali, C. Del Papa, B. Esposito, P. Giusti,
T. Massam, R. Nania, G. Natale, F. Palmonari, G. Sartorelli,
M. Spinetti, G. Susinno, L. Votano and A. Zichichi

CERN, Geneva, Switzerland
Istituto di Fisica dell'Università di Bologna, Italy
Istituto Nazionale di Fisica Nucleare, Bologna, Italy
Istituto Nazionale di Fisica Nucleare, LNF, Frascati, Italy

(Presented by A. Zichichi)

1. INTRODUCTORY NOTES

I would like to contribute just two points to the discussion of hadron colliders versus e^+e^- colliders. Both will be based on experimental data observed at the ISR and extrapolated at extreme energies. The first is in the field of new, very heavy flavours; the second is on the multiparticle production. Both could contribute to changing our present views and to favouring, for the future, very high energy hadron colliders -- not (e^+e^-).

1) A very high energy hadron collider exists: the CERN $(p\bar{p})$. Can this machine be used to search for new flavours such as "top" at 25 GeV and "superbeauty" at 55 GeV masses? The answer is Yes if the production mechanism and other detailed features follow our expectations.

A detailed account of how this can be done has been given during another session [1]. Let me just remind you of the crucial points.

A study of a new effect (the e^+/e^- asymmetry in the proton and antiproton hemispheres) shows that it is possible to search for very heavy flavour states. This new effect depends on the $e^{\pm}$ energy and is there if the very heavy states (Λ^+_t and $\Lambda^0_{\text{superbeauty}}$) are produced in a leading

way, as found at the CERN ISR energies with "charm" and "beauty" [2,3]. If these states were found at the CERN $p\bar{p}$ Collider, this would be a very important step in favour of hadron machines. In fact it could be that the 25 GeV and 55 GeV masses decay semileptonically in a pattern which is simple to disentangle from the "standard" soft physics produced in a very high energy interaction.

On the basis of this detailed study we think that the observation of new flavours in hadron colliders is by no means out of reach.

Of course the great advantage of e^+e^- colliders is that they are "clean". However their energy is much below that of the hadron colliders.

If the hadron colliders will show that, after all, they are not so difficult to work with, and the complexity of the final states is not such as to forbid doing new physics -- for example, to discover new flavours -- in few years our view could drastically change in favour of them.

So the first conclusion is to wait until a clear message comes from the CERN $p\bar{p}$ Collider.

2) The second point refers to a new way of studying (pp) interactions.

I will discuss this second point in detail. In fact, this new way of studying (pp) interactions allows a comparison of the multiparticle systems produced in a hadron collider (such as the ISR) with the multiparticle systems produced in a lepton collider (such as PETRA).

In other words, in so far as the multiparticle hadronic states are concerned, the ISR looks like an e^+e^- collider, whose energy goes beyond the highest PETRA values. There is a difference between (e^+e^-) and hadron machines: the production of open and hidden heavy-flavour states. This difference can easily be accounted for in terms of the couplings which are just given by the up-like or down-like electric charges in the e^+e^- colliders, whilst in the hadron case the mass of the heavy flavours comes in with an inverse power law. But the structure of the multibody final states looks very similar at the ISR and at PETRA. Moreover, if a lepton-hadron collider would be built at equivalent ISR energies, the structure of the multibody final states would be identical, as shown by the comparison of the lowest-energy ISR data with the highest-energy (νp), $(\bar{\nu}p)$, and (μp) scattering data.

A direct consequence of these findings is that an old myth has been shattered.

2. THE END OF A MYTH: THE HIGH-p_T PHYSICS

2.1 General remarks

So far, the high-p_T physics has had a highly privileged role in hadron phenomena. For example, high-p_T hadron physics was the only candidate to attempt a comparison with (e^+e^-) physics and deep-inelastic scattering (DIS) [4]. This trend has been continuing for a long time.

Recently, the advent of QCD has emphasized this privileged role of the high-p_T physics [5-7]. The reason is very simple: at high p_T, thanks to asymptotic freedom, QCD calculations can be attempted via perturbative methods, and can be successfully confronted with experimental data. The new CERN $p\bar{p}$ Collider results are indeed the latest successful attempt in this trend [8-10].

On the contrary, low-p_T phenomena are "theoretically off limits", despite the fact that they represent an overwhelming amount of experimental data.

In a long series of systematic studies at the ISR on the properties of multiparticle hadronic systems produced in low-p_T (pp) interactions, we have discovered a remarkable set of analogies between the properties of the multiparticle system produced in low-p_T (pp) interactions, (e^+e^-) annihilation, and in DIS processes [11-27].

The key point in these studies is the new method introduced in order to study (pp) interactions at the ISR. This method is based on the subtraction of the "leading" proton effect from the final state of a (pp) interaction. Once the "leading" protons are subtracted, it is possible to work in the correct reference frame of the multiparticle system produced. Moreover, it is possible to calculate the "effective" energy available for particle production, defined as

$$\sqrt{(q_{tot}^{had})^2} = \sqrt{(q_1^{inc} + q_2^{inc} - q_1^{leading} - q_2^{leading})^2} \quad , \qquad (1)$$

where $q_{1,2}^{inc}$ and $q_{1,2}^{leading}$ are the four-vectors of the incident and "leading" protons, respectively.

This "effective" energy can be very different from the "nominal" total energy of the ISR proton beams.

Let us point out that the "leading" proton effect (see Fig. 1) is not a phenomenon limited to the ISR case -- nor to the proton-proton collisions [28,29]. We have investigated this phenomenon and have discovered that the "leading" hadron effect is present no matter if the interaction is initiated by a hadron signal, or by a photon, or by a weak boson (see Fig. 2). Moreover, we have found that the "leading" effect is more pronounced when more "quarks" are allowed to go from the initial to the final state (see Fig. 1). These findings imply that our new method of investigating multiparticle hadronic systems produced in (pp) interactions at the ISR is indeed of general validity, and should be used in all reactions in order to establish a common and understood basis for their comparison. It is manifestly incorrect to compare processes where the "effective" energy available for particle production is not the same.

This means that it is wrong to compare, for example, the multiparticle hadronic systems produced in a (pp) collision at $(\sqrt{s})_{pp}$ = 30 GeV with the multiparticle hadronic systems produced in a (e^+e^-) annihilation at $(\sqrt{s})_{e^+e^-}$ = 30 GeV. In fact $(\sqrt{s})_{pp}$ is not the "effective" energy available for particle production, whilst $(\sqrt{s})_{e^+e^-}$ is (see Fig. 3). In a (pp) interaction the effective energy available for particle production is $\sqrt{(q^{had}_{tot})^2}$, as shown in formula (1).

An analogous problem exists in the DIS case. Here the quantity W, defined as the total energy of the hadronic system, does indeed contain a "leading" hadron. This is the reason why the average charged-particle multiplicities measured in DIS and in (e^+e^-) could not agree (see Fig. 4). The multiparticle hadronic system, produced in (e^+e^-) and (DIS) can be compared, on a sound basis, only if $(\sqrt{s})_{e^+e^-}$ is compared not with W but with $\sqrt{(q^{had}_{tot})^2}$.

2.2 The identification of the correct variables

The identification of the correct variables in describing hadron production in (pp) interactions, (e^+e^-) annihilation, and DIS processes, is the basic starting point for studying analogies among and differences between these three ways of producing multiparticle hadronic systems.

Let me show how this is done.

2.2.1 e^+e^- annihilation is illustrated in the following diagram:

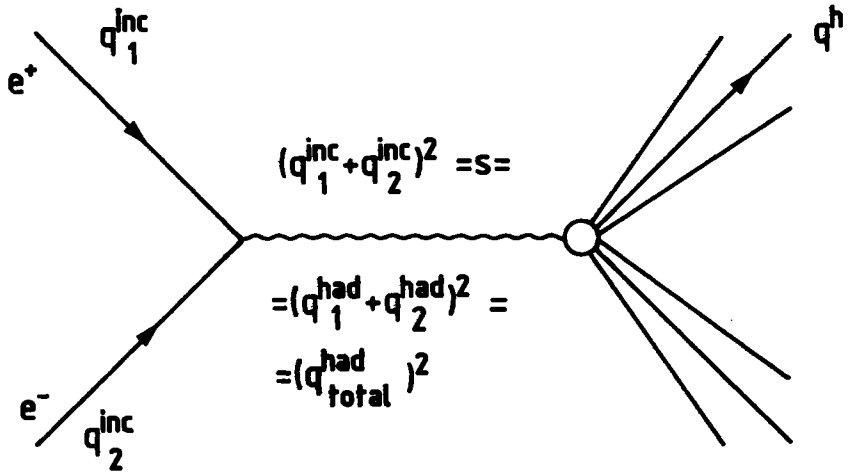

where q_1^{inc} and q_2^{inc} are the four-momenta of the incident electron e^- and positron e^+; q^h is the four-momentum of a hadron produced in the final state, whose total energy is

$$(\sqrt{s})_{e^+e^-} = \sqrt{(q_1^{inc} + q_2^{inc})^2} = 2E_{beam} \qquad (2)$$

(when the colliding beams have the same energy).

As we will see later,

$$q_1^{inc} = q_1^{had} ,$$

$$q_2^{inc} = q_2^{had} ,$$

where $q_{1,2}^{had}$ are the four-momenta available in a (pp) collision for the production of a final state with total hadronic energy

$$\sqrt{(q_1^{had} + q_2^{had})^2} = \sqrt{(q_{tot}^{had})^2} . \qquad (3)$$

It is this quantity $\sqrt{(q_{tot}^{had})^2}$ which should be used in the comparison with (e^+e^-) annihilation, and therefore with

$$(\sqrt{s})_{e^+e^-} \qquad (4)$$

This means that

$$(\sqrt{s})_{e^+e^-} = \sqrt{(q_{tot}^{had})^2} \quad . \tag{5}$$

Moreover, the fractional energy of a hadron produced in the final state of an (e^+e^-) annihilation is given by

$$(x)_{e^+e^-} = 2\,\frac{q^h \cdot q_{tot}^{had}}{q_{tot}^{had} \cdot q_{tot}^{had}} = 2\,\frac{E^h}{(\sqrt{s})_{e^+e^-}}$$

where the dots indicate the scalar product and E^h is the energy of the hadron "h" measured in the (e^+e^-) c.m. system. Notice that the four-momentum q_{tot}^{had} has no space-like part:

$$q_{tot}^{had} \equiv \left[i\vec{0};\ (\sqrt{s})_{e^+e^-} \right] .$$

2.2.2 DIS processes are illustrated in the diagram below:

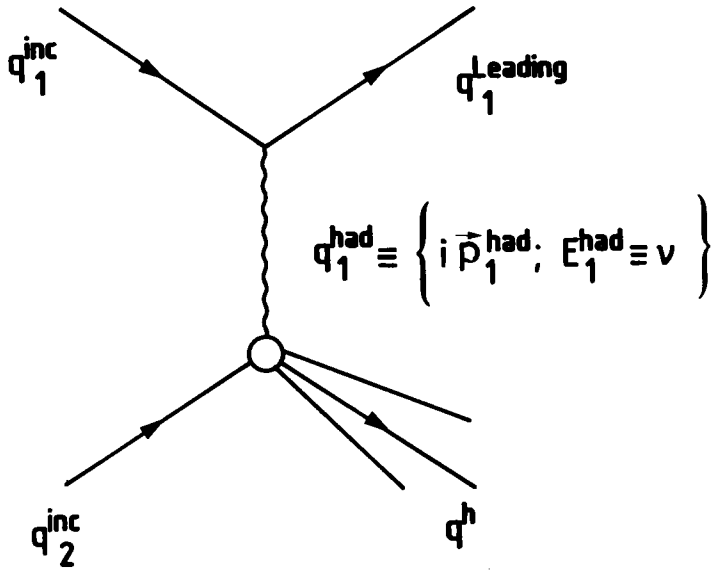

where q_1^{inc} and $q_1^{leading}$ are the four-momenta of the initial- and final-state leptons, respectively; q_2^{inc} is the four-momentum of the target nucleon; q_1^{had} is the four-momentum transferred from the leptonic to the hadronic vertex whose time-like component is usually indicated as ν:

$$q_1^{had} \equiv (i\vec{p}_1^{\,had};\quad \nu \equiv E_1^{had}) \ .$$

Notice that in order to easily identify the equivalent variables in (pp) interactions, we have introduced a notation in terms of E_1^{had} and $\vec{p}_1^{\,had}$.

A basic quantity in DIS is the total hadronic mass

$$(W^2)_{DIS} = (q_1^{had} + q_2^{inc})^2$$

and the fractional energy

$$(z)_{DIS} = \frac{q^h \cdot q_2^{inc}}{q_1^{had} \cdot q_2^{inc}} \ ,$$

where again the dots between the four-momenta indicate their scalar product.

2.2.3 (pp) interactions are illustrated in the following graph:

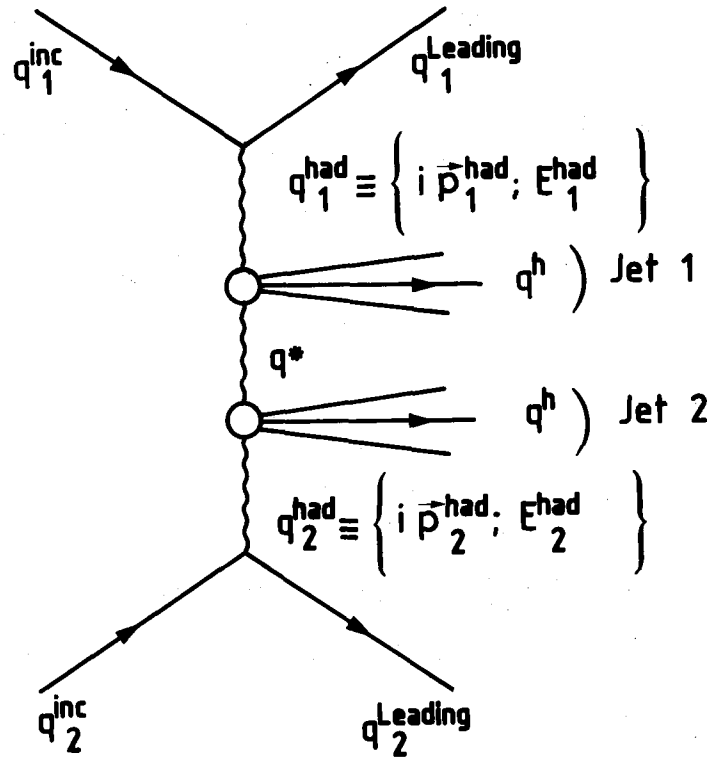

where $q_{1,2}^{inc}$ are the four-momenta of the two incident protons; $q_{1,2}^{leading}$ are the four-momenta of the two leading protons; $q_{1,2}^{had}$ are the space-like four-momenta emitted by the two proton vertices; q^h is the four-momentum of a hadron produced in the final state.

Now, attention! A (pp) collision can be analysed in such a way as to produce the key quantities proper to (e^+e^-) annihilation and DIS processes.

In fact, from the above diagram we can work out the following quantities*), which are needed if we want to compare (pp) physics with (e^+e^-), i.e.

$$(q_{tot}^{had})_{pp} = (q_1^{had} + q_2^{had})_{pp} ;$$

in fact

$$\sqrt{(q_{tot}^{had})^2}_{pp} = (\sqrt{s})_{e^+e^-} .$$

Moreover,

$$(x)_{pp}^{had} = 2 \frac{q^h \cdot q_{tot}^{had}}{q_{tot}^{had} \cdot q_{tot}^{had}} ,$$

to be compared with

$$(x)_{e^+e^-}^{had} = 2 \frac{q^h \cdot (q_{tot}^{had})_{e^+e^-}}{(q_{tot}^{had})_{e^+e^-} \cdot (q_{tot}^{had})_{e^+e^-}} ,$$

where the subscripts (e^+e^-) in q_{tot}^{had} are there to make it clear that these quantities are measured in (e^+e^-) collisions and are the quantities equivalent to q_{tot}^{had} measured in (pp) interactions.

The same (pp) diagram shown above can be used in order to work out the key quantities needed when we want to compare (pp) physics with DIS. In this case we have

---

*) Notice that: $\sqrt{(q_{tot}^{had})^2} \simeq 2E^{had}$, and $(x)_{pp}^{had} \simeq x_R^*$.

$$(W^2)^{had}_{pp} = (q_1^{had} + q_2^{inc})^2$$

and

$$(z)^{had}_{pp} = \frac{q^h \cdot q_2^{inc}}{q_1^{had} \cdot q_2^{inc}} .$$

Notice that in W^2 the leading proton No. 2 is not subtracted. This is the reason for the differences found in the comparison between DIS data and e^+e^- (see Fig. 4). In fact (W^2) is not the effective total energy available for particle production, owing to the presence there of the leading proton.

2.3 Experimental results

A series of experimental results, where (pp) interactions have been analysed *à la* e^+e^- and *à la* DIS, have given impressive analogies in the multiparticle systems produced in these -- so far considered -- basically different processes: (pp), (e^+e^-), DIS.

The experimental data where (pp) interactions are compared with (e^+e^-) are shown in Figs. 5-12.

The experimental data where (pp) interactions are compared with DIS are shown in Figs. 13-15.

These comparisons show striking analogies with respect to the following quantities:

i) the inclusive fractional energy distribution of the produced particles [11,12,19,21] (see Figs. 5,6,15);

ii) the average charged-particle multiplicities [13,18,22,26,27] (see Figs. 7,13,14);

iii) the ratio of the average energy associated with the charged particles over the total energy available for particle production [15] (see Fig. 8);

iv) the inclusive transverse momentum distribution of the produced particles [17,20] (see Figs. 9-11);

v) the correlation functions in rapidity [25] (see Fig. 12);

Notice the power of the (pp) interaction. Once this is analysed in the correct way it produces results equivalent to (e^+e^-) and DIS.

This means that there is an important universality governing these -- so far considered -- different ways of producing multihadronic systems.

2.4 Conclusions

From the above analysis we can conclude that

1) the leading effect must be subtracted if we want to compare purely hadronic interactions with (e^+e^-) and DIS;

2) the old myth, based on the belief that in order to compare (pp) with (e^+e^-) and DIS you need high-p_T (pp) interactions, is dead. In fact we have proved that low-p_T (pp) interactions produce results in excellent analogy with (e^+e^-) annihilation and DIS processes, the basic parameter in (pp) interactions being $\sqrt{(q^{had}_{tot})^2}$ for a comparison with (e^+e^-), and $\sqrt{W^2_{(pp)}}$ for a comparison with DIS.

   The existence of high-p_T events means that point-like constituents exist inside the nucleon. But low-p_T events contain the same amount of basic information as high-p_T events. No special features -- apart from $\langle p_T \rangle$ [see point (3) below] -- should emerge in the high-p_T events because low-p_T events follow (e^+e^-) and DIS.

3) Now two extrapolations:

   There are two ways of producing $\sqrt{(q^{had}_{tot})^2}$:

   i) one is at low p_T, and we have seen what happens;

   ii) the other is at high p_T: we have not been able to compare, at constant values of $\sqrt{(q^{had})^2_{tot}}$, the multiparticle systems produced in (pp) interactions at high p_T and at low p_T.

   Our analysis of the inclusive transverse momentum distribution, in terms of the renormalized variable $p_T/\langle p_T \rangle$ [notice that here p_T indicates the transverse momentum of the particles produced with respect to the jet axis, not to the colliding (pp) or $(p\bar{p})$ axis], is suggestive of a very interesting possibility: i.e. multiparticle systems produced at high p_T could show, at equivalent $\sqrt{(q^{had})^2_{tot}}$, higher values of $\langle p_T \rangle$. This would mean that high-p_T multiparticle systems are produced by heavy quarks.

An extrapolation of our method to the CERN $p\bar{p}$ Collider would allow a large energy jump and could produce clear evidence for heavy quark production.

Let us give an example. If two jets at the $p\bar{p}$ Collider are produced back-to-back with the same transverse energy E_T, then we have

$$\sqrt{(q_{tot}^{had})^2} \cong 2E_T \ .$$

Suppose that we are at

$$2E_T = 100 \text{ GeV} \ .$$

This system, according to our extrapolation, should be like a multiparticle state produced by $(\sqrt{s})_{e^+e^-} = 100$ GeV.

The key point is to see if, at the CERN $p\bar{p}$ Collider, a multiparticle system produced at low p_T but with

$$\sqrt{(q_{tot}^{had})^2} = 100 \text{ GeV}$$

looks like the one produced at high E_T. The main difference we can expect is the value of $\langle p_T \rangle$.

To check these points is another important contribution in order to understand how hadron colliders compare with e^+e^- colliders.

3. CONCLUSIONS

1) The new way of exploiting the CERN $p\bar{p}$ Collider could bring about a serious competition with the (e^+e^-) colliders in a very important field: the search for new flavours at very high masses.

2) The new method of studying (pp) and $(p\bar{p})$ collisions -- based on the subtraction of the "leading" effects -- allows us to put on equal footing the multiparticle systems that are produced in purely hadronic interactions, in (e^+e^-) annihilation, and in DIS processes.
Purely hadronic interactions means using machines such as the ISR, the CERN $p\bar{p}$ Collider, the BNL-CBA Collider, and the Fermilab $(p\bar{p})$ Collider.

(e^+e^-) annihilation means using machines such as LEP and its possible developments.

DIS processes means using machines such as HERA.

The "leading" subtraction allows us to show that a universal feature is at work in the mechanism, which produces multibody final states in (pp), (e^+e^-), and DIS.

So, in the field of new, very heavy flavours, and of multiparticle production, our views on hadron colliders could change in the near future. The crucial machine is the CERN $p\bar{p}$ Collider.

REFERENCES

[1] A. Zichichi, New flavours: experiment versus theory. From charm to the 4th family, Talk given at this conference.

[2] M. Basile et al., Nuovo Cimento Letters 30, 487 (1981).

[3] M. Basile et al., Nuovo Cimento 65A, 408 (1981).

[4] M. Jacob and P.V. Landshoff, Phys. Rep. 48, No. 4 (1978).

[5] E. Reya, Phys. Rep. 69, No. 3 (1981).

[6] P.V. Landshoff, Testing QCD in hadronic processes, Lecture given at the "Ettore Majorana" Int. School of Subnuclear Physics, Erice, 1982.

[7] M. Jacob, CERN-TH/3515 (1983)

[8] UA2 Collaboration, Phys. Lett. B118, 203 (1982).

[9] UA1 Collaboration, preprint CERN-EP/83-02 (1983).

[10] H. Boggild, CERN-EP/82-187 (1982).

[11] M. Basile et al., Phys. Lett. 92B, 367 (1980).

[12] M. Basile et al., Nuovo Cimento 58A, 193 (1980).

[13] M. Basile et al., Phys. Lett. 95B, 311 (1980).

[14] M. Basile et al., Nuovo Cimento Lett. 29, 491 (1980).

[15] M. Basile et al., Phys. Lett. 99B, 247 (1981).

[16] M. Basile et al., Nuovo Cimento Lett. 30, 389 (1981).

[17] M. Basile et al., Nuovo Cimento Lett. 31, 273 (1981).

[18] M. Basile et al., Nuovo Cimento 65A, 400 (1981).

[19] M. Basile et al., Nuovo Cimento 65A, 414 (1981).

[20] M. Basile et al., Nuovo Cimento Lett. 32, 210 (1981).

[21] M. Basile et al., Nuovo Cimento 67A, 53 (1982).

[22] M. Basile et al., Nuovo Cimento 67A, 244 (1982).

[23] M. Basile et al., preprint CERN-EP/81-147 (1981).

[24] M. Basile et al., preprint CERN-EP/82-182 (1982), submitted to Nuovo Cimento.

[25] G. Bonvicini et al., preprint CERN-EP/83-29 (1983), submitted to Nuovo Cimento Letters.

[26] M. Basile et al., Nuovo Cimento Letters 36, 303 (1983).

[27] G. Bonvicini et al., preprint CERN-EP/83-33 (1983), submitted to Nuovo Cimento Letters.

[28] M. Basile et al., Nuovo Cimento 66A, 129 (1981).

[29] M. Basile et al., Nuovo Cimento Letters 32, 321 (1981).

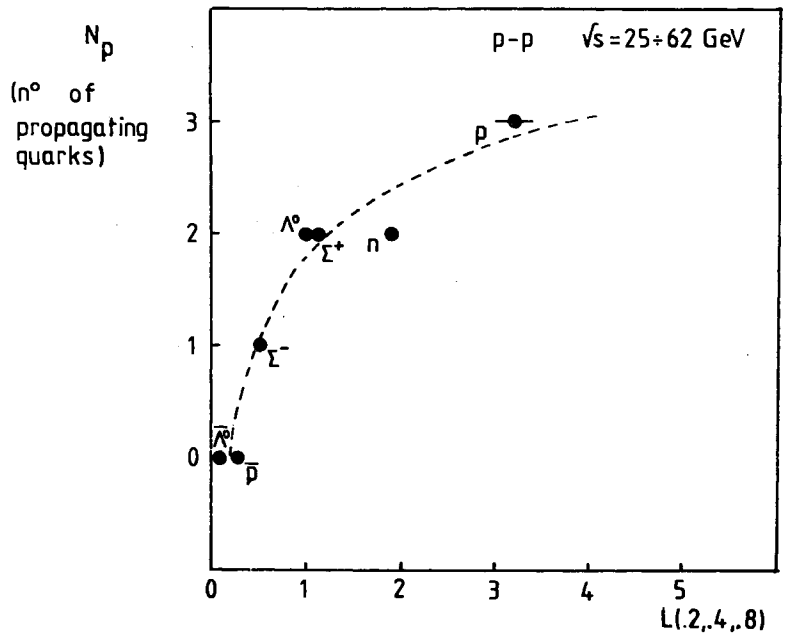

Fig. 1 The leading quantity L(0.2, 0.4, 0.8), for various final-state hadrons in (pp) collisions at ISR energies (25 to 62 GeV), is plotted versus the number of propagating quarks from the incoming into the final-state hadrons. $L(x_0,x_1,x_2)$ is defined as $L(x_0,x_1,x_2) = \int_{x_1}^{x_2} F(x)dx / \int_{x_0}^{x_1} F(x)dx$, where $F(x) = (1/\pi)\int\left[(2E/\sqrt{s})(d^2\sigma/dx dp_T^2)\right]dp_T^2$. The dashed line is obtained by using a parametrization of the single-particle inclusive cross-section, as described in Refs. 28 and 29.

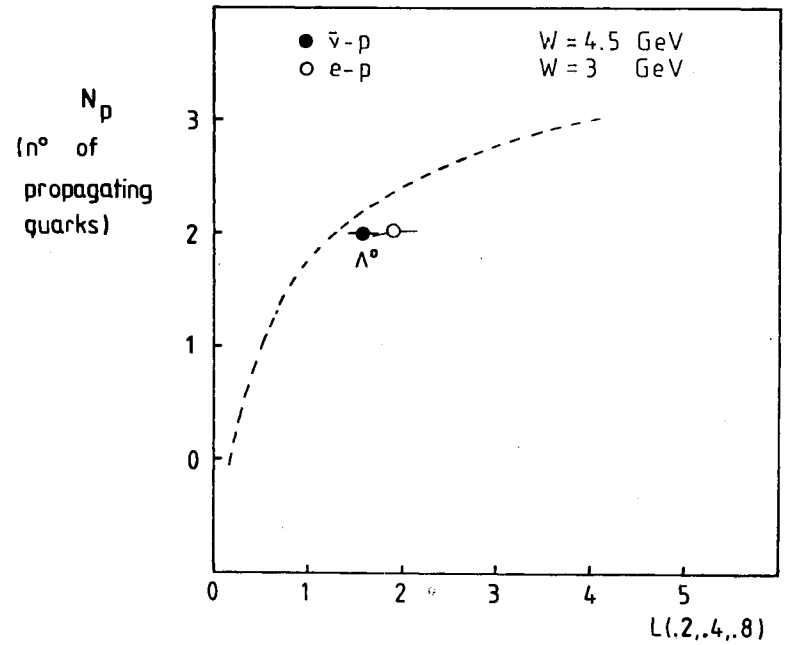

Fig. 2 L(0.2, 0.4, 0.8) for Λ^0 production in ($\bar{\nu}$p) and (ep) reactions. The dashed line is the same as for Fig. 1.

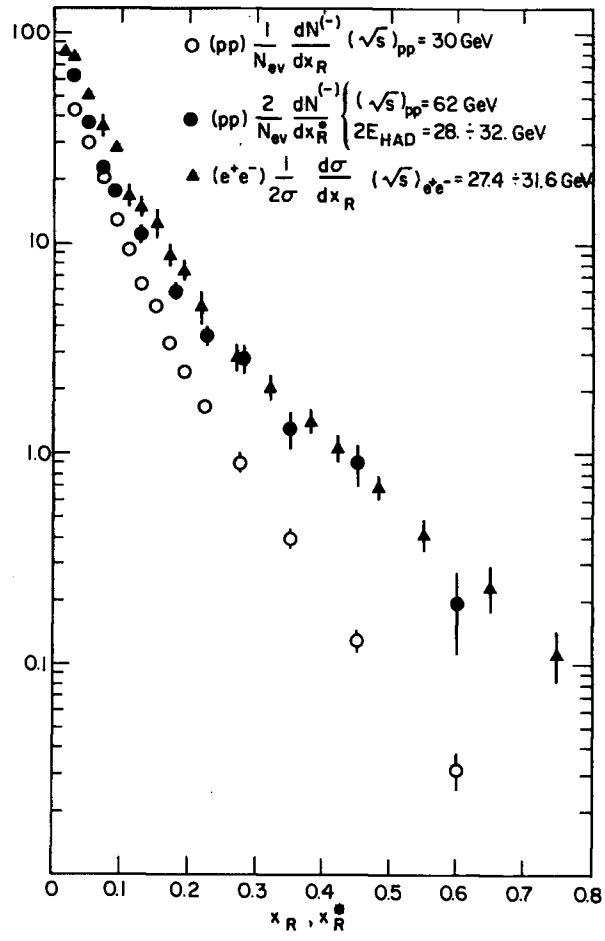

Fig. 3 The inclusive fractional momentum distributions of negative particles for (pp) interactions using the standard analysis at $(\sqrt{s})_{pp}$ = 30 GeV (open points); using the method of removing the leading protons at $(\sqrt{s})_{pp}$ = 62 GeV and 2Ehad = 28 to 32 GeV (black circles); the (e^+e^-) data at $(\sqrt{s})_{e^+e^-}$ = 27.4 to 31.6 GeV (black triangles).

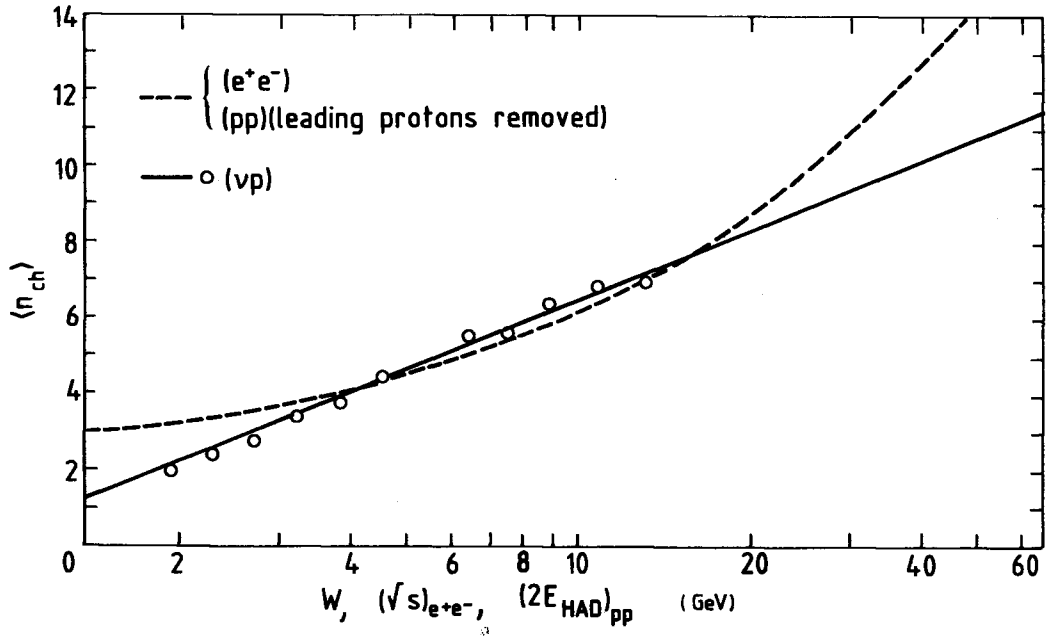

Fig. 4 The dashed line is the best fit to $\langle n_{ch} \rangle$ measured in (e^+e^-) versus $(\sqrt{s})_{e^+e^-}$, and in (pp) removing leading protons versus 2Ehad. The points are the measurements of $\langle n_{ch} \rangle$ versus W in (νp) DIS, and the continuous line is the best fit to these data.

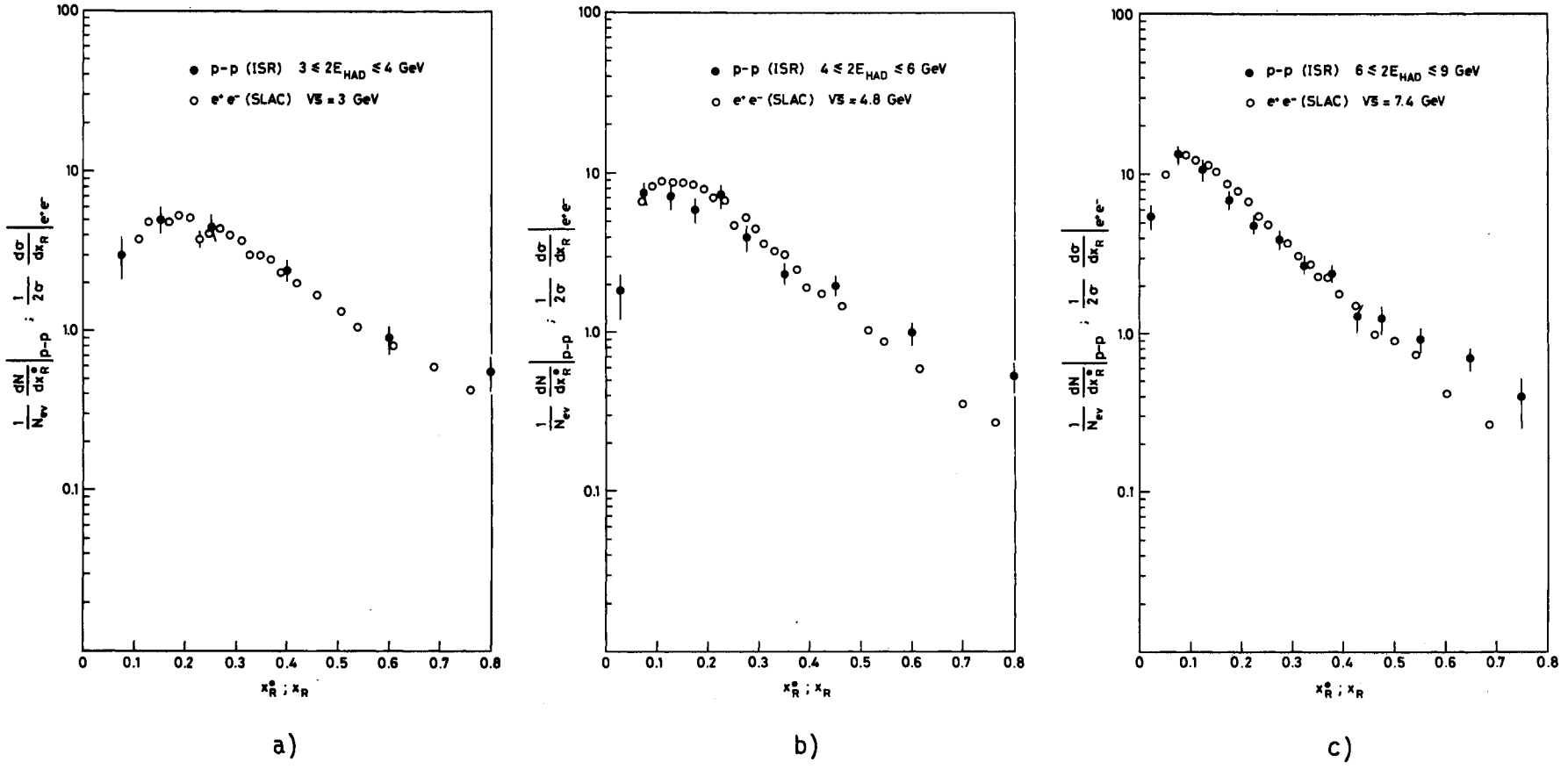

Fig. 5 The inclusive single-particle fractional momentum distributions $(1/N_{ev})(dN_{track}/dx_R^*)$ for data taken at $(\sqrt{s})_{pp}$ = 30 GeV and for three intervals of $2E^{had}$. Also shown are data from SPEAR.

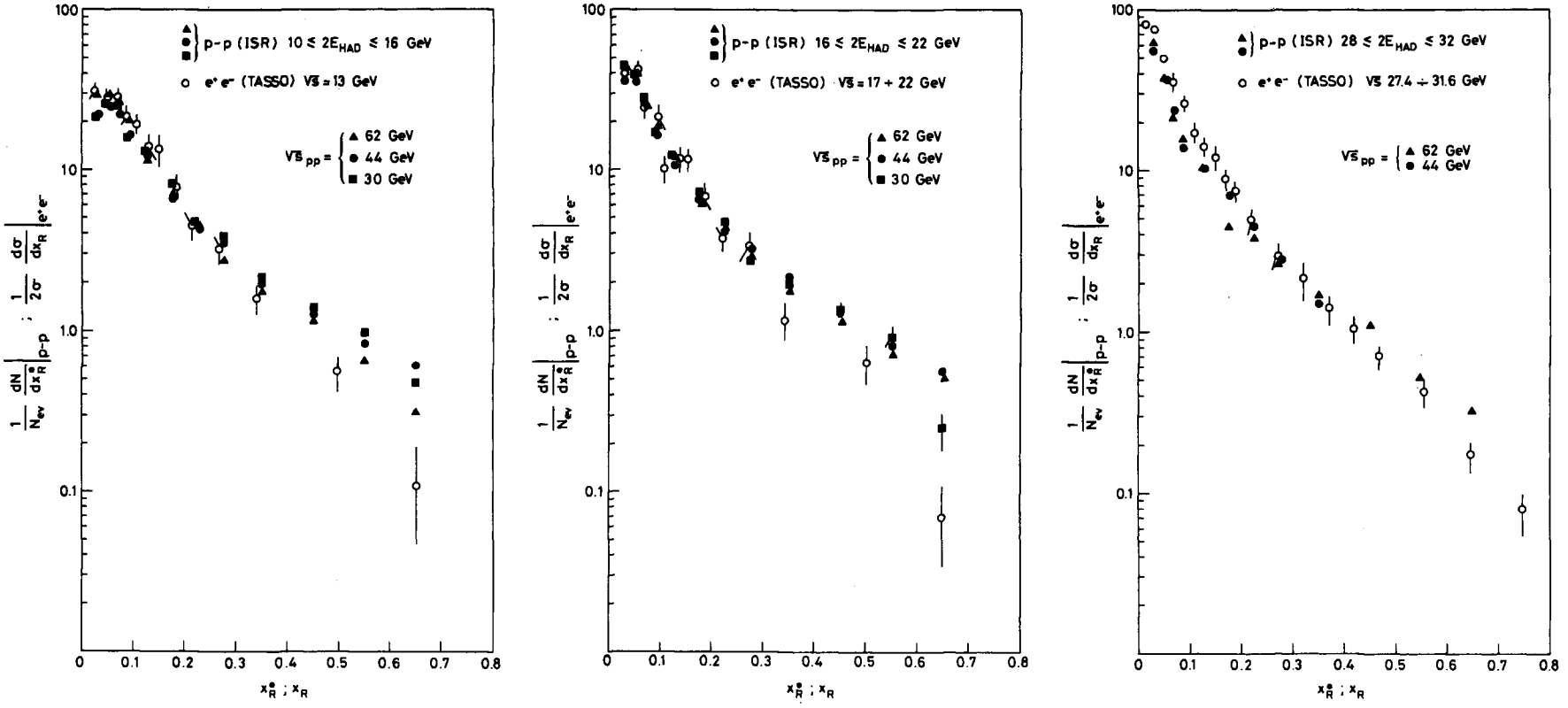

Fig. 6 The inclusive single-particle fractional momentum distributions $(1/N_{ev})(dN_{track}/dx_R^*)$ in the same $2E^{had}$ interval, but different $(\sqrt{s})_{pp}$. Also shown are data from TASSO at PETRA.

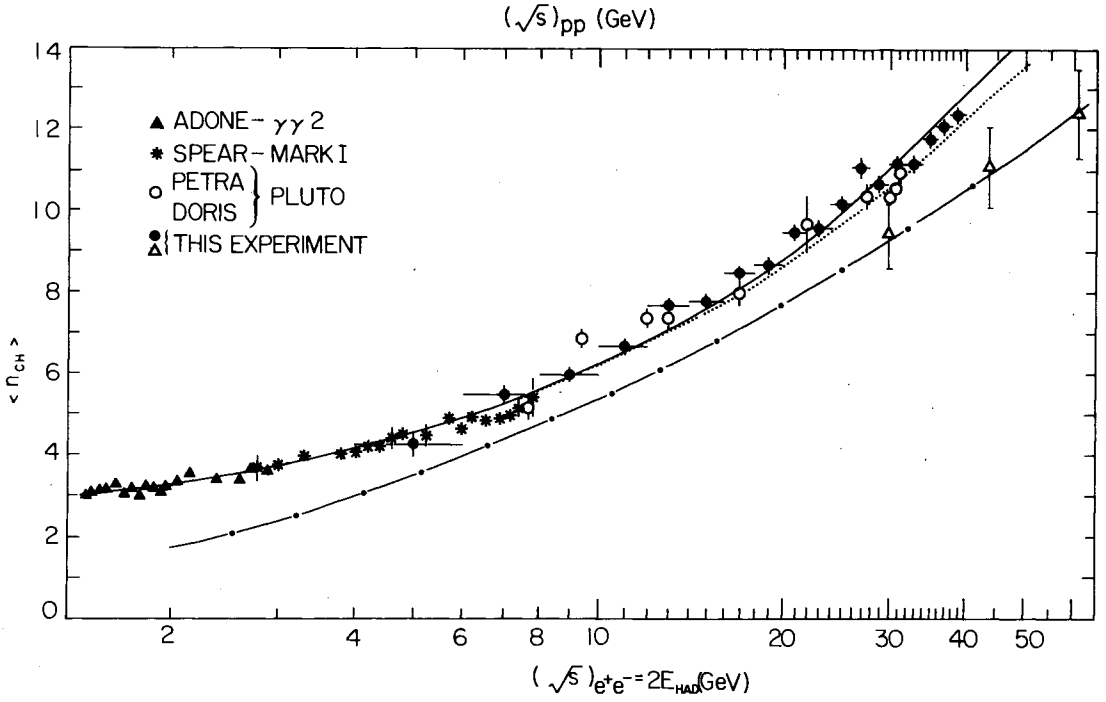

Fig. 7 Mean charged-particle multiplicity [averaged over different $(\sqrt{s})_{pp}$] versus $2E^{had}$, compared with (e^+e^-) data. The continuous line is the best fit to our data according to the formula $\langle n_{ch} \rangle = a + b \exp\left[c\sqrt{\ln (s/\Lambda^2)}\right]$. The dotted line is the best fit using PLUTO data. The dashed-dotted line is the standard (pp) total charged-particle multiplicity with, superimposed, our data as open triangular points.

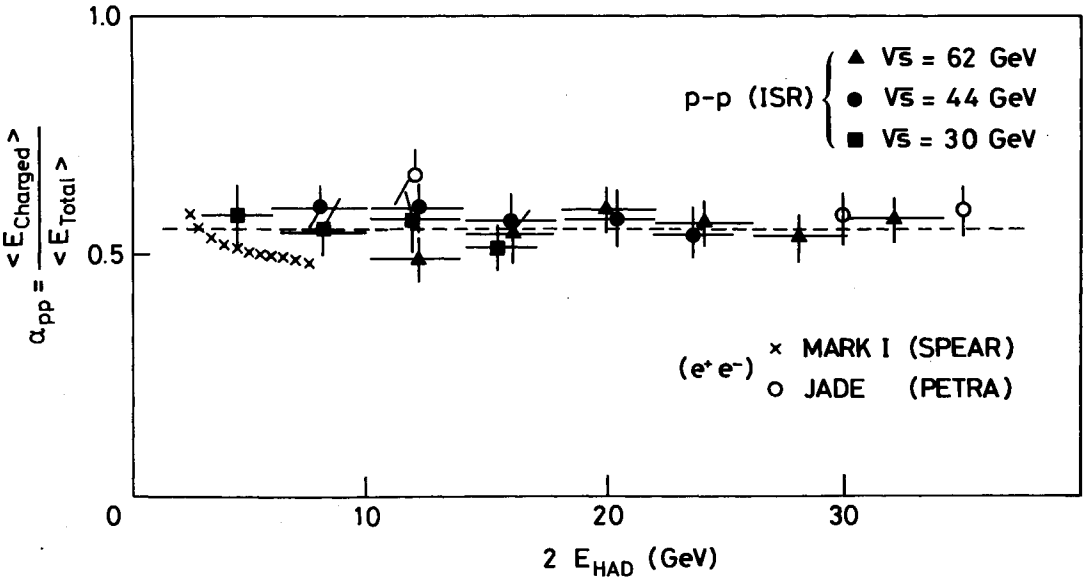

Fig. 8 The charged-to-total energy ratio obtained in (pp) collisions α_{pp}, plotted versus $2E^{had}$ and compared with (e^+e^-) obtained at SPEAR and PETRA.

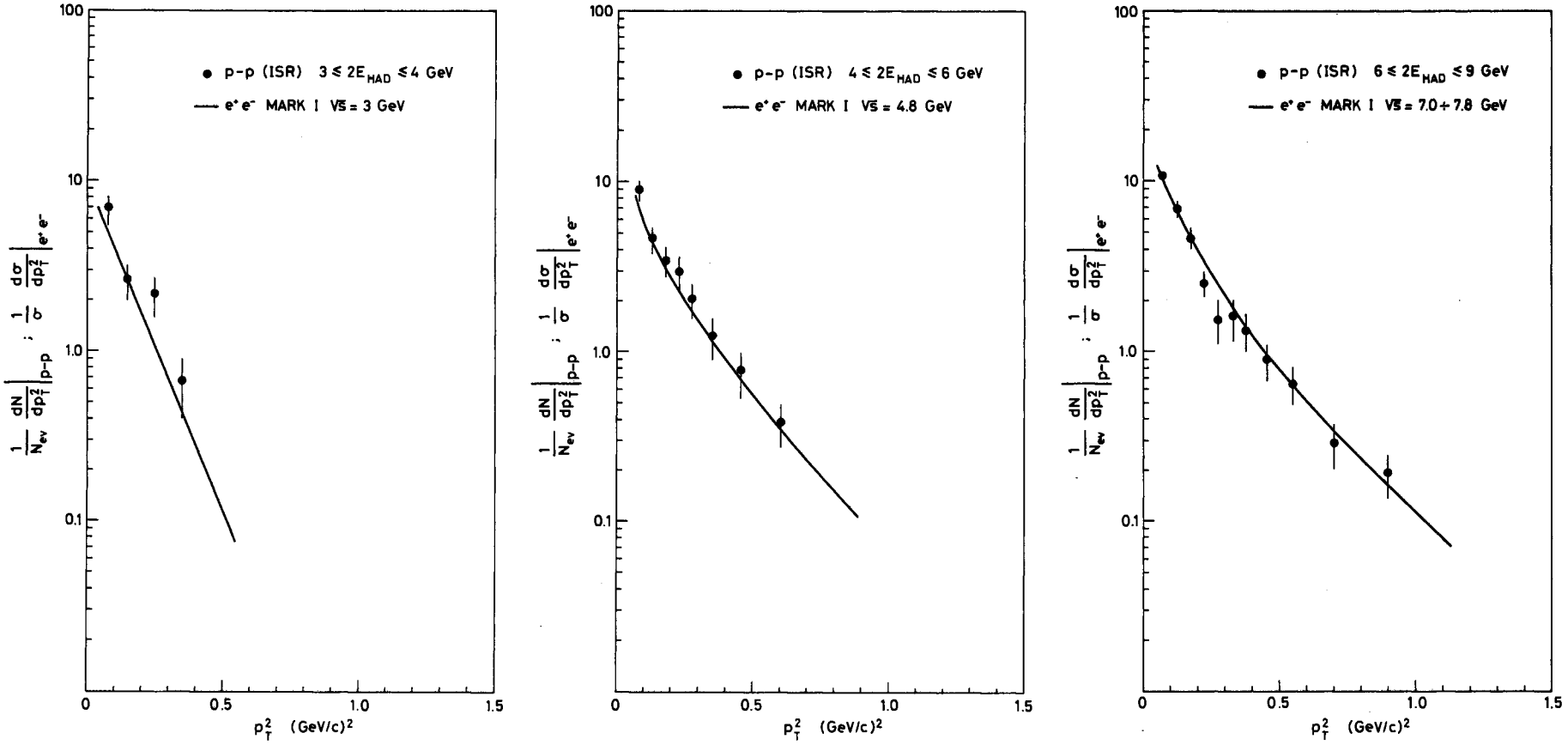

Fig. 9 The inclusive single-particle transverse momentum distribution $(1/N_{ev})(dN_{track}/dp_T^2)$ for data taken at $(\sqrt{s})_{pp}$ = 30 GeV and for three intervals of $2E^{had}$. Also shown is the fit to the SPEAR data (continuous line).

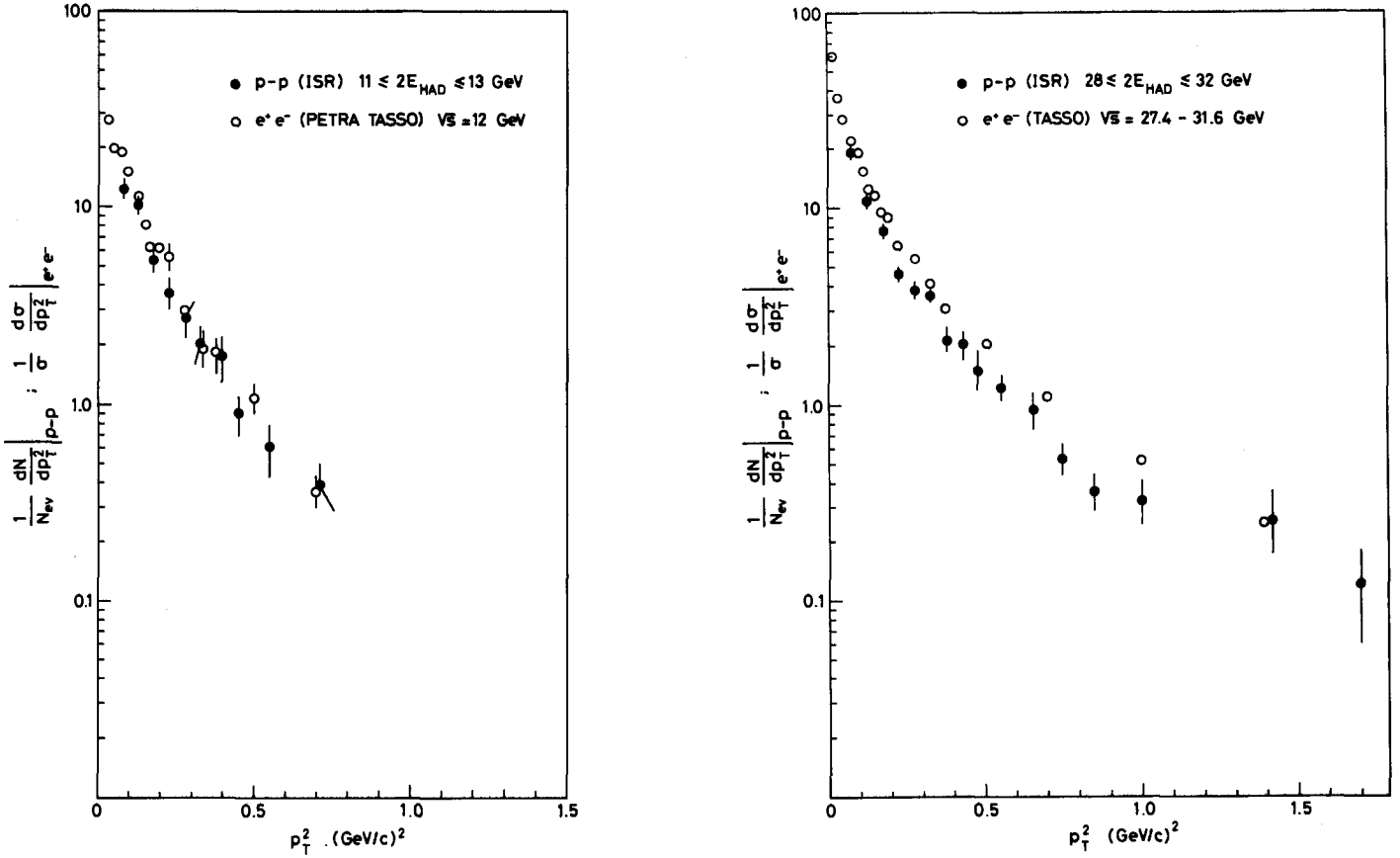

Fig. 10 The inclusive single-particle transverse momentum distributions $(1/N_{ev})(dN_{track}/dp_T^2)$ for two E^{had} range. Also shown are data from TASSO at PETRA.

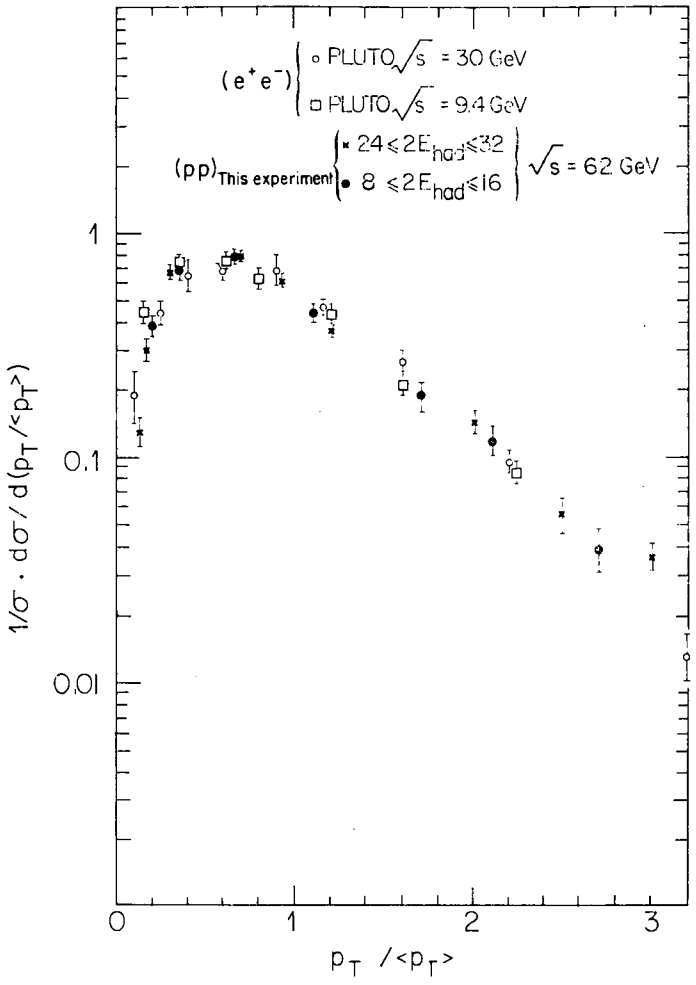

Fig. 11 The differential cross-section $(1/\sigma)[d\sigma/d(p_T/\langle p_T\rangle)]$ versus the "reduced" variable $p_T/\langle p_T\rangle$. These distributions allow a comparison of the multiparticle systems produced in (e^+e^-) annihilation and in (pp) interactions in terms of the renormalized transverse momentum properties.

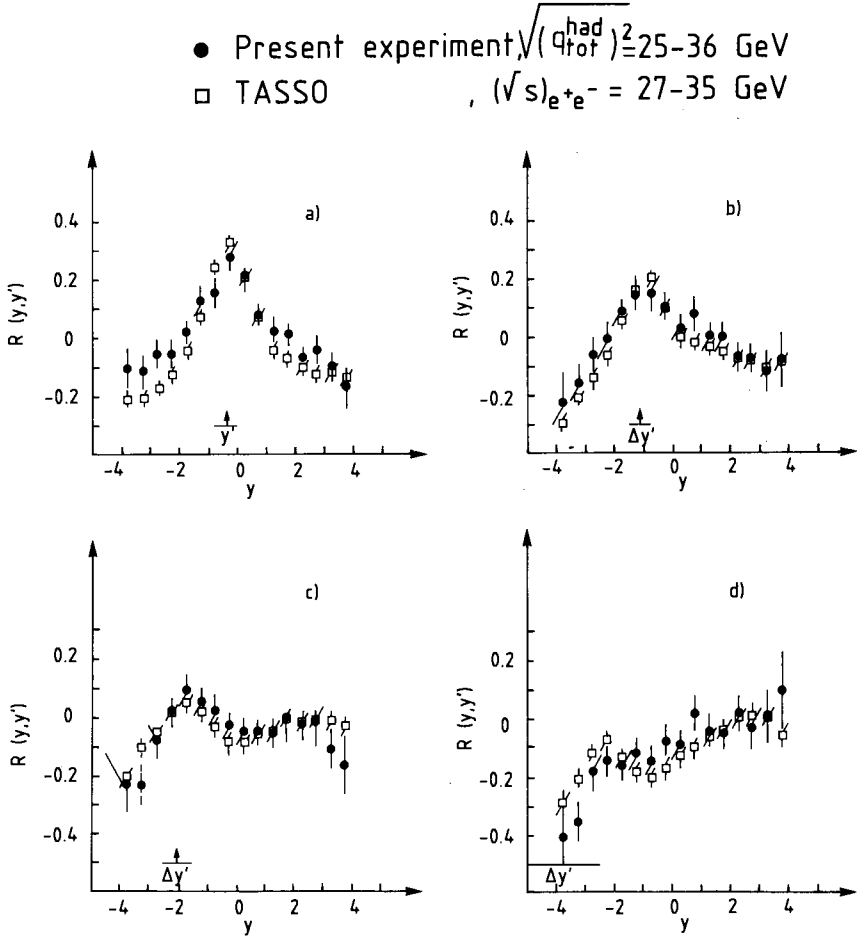

Fig. 12 Two-particle correlation in rapidity space: $R(y,y')$, for different y' intervals, as measured in the present experiment after the leading proton subtraction in the $\sqrt{(q^{had}_{tot})^2}$ range 25 to 36 GeV (black points), compared with the results by the TASSO Collaboration at $(\sqrt{s})_{e+e-}$ between 27 and 35 GeV (open squares).

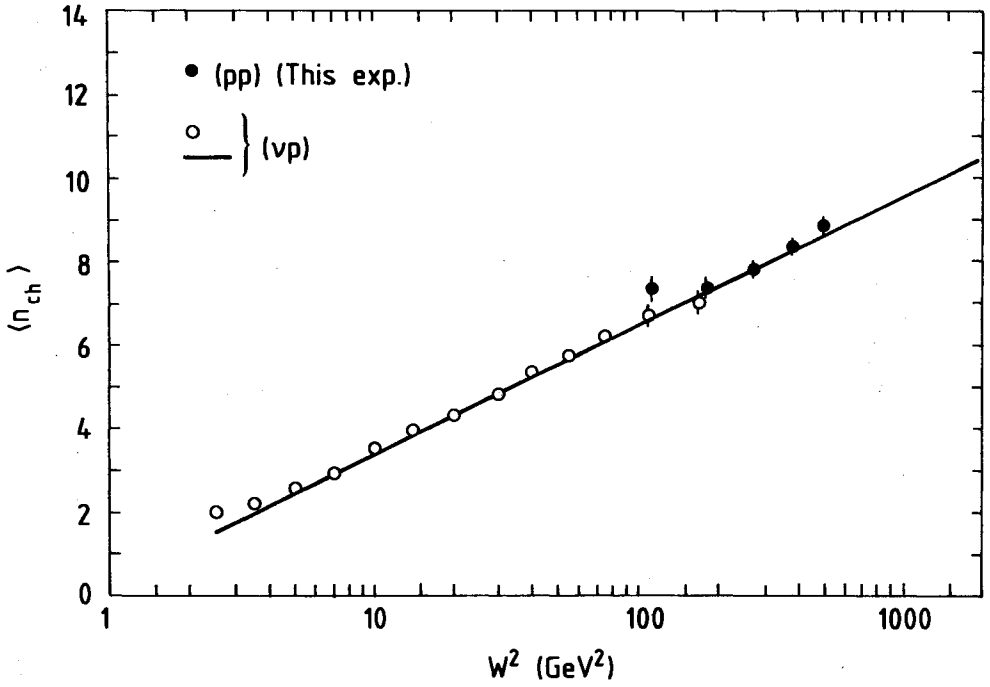

Fig. 13 The average charged-particle multiplicities $\langle n_{ch} \rangle$ measured in (pp) at $(\sqrt{s})_{pp}$ = 30 GeV, using a DIS-like analysis, are plotted versus W^2 (black points). The open points are the (νp) data and the continuous line is their best fit.

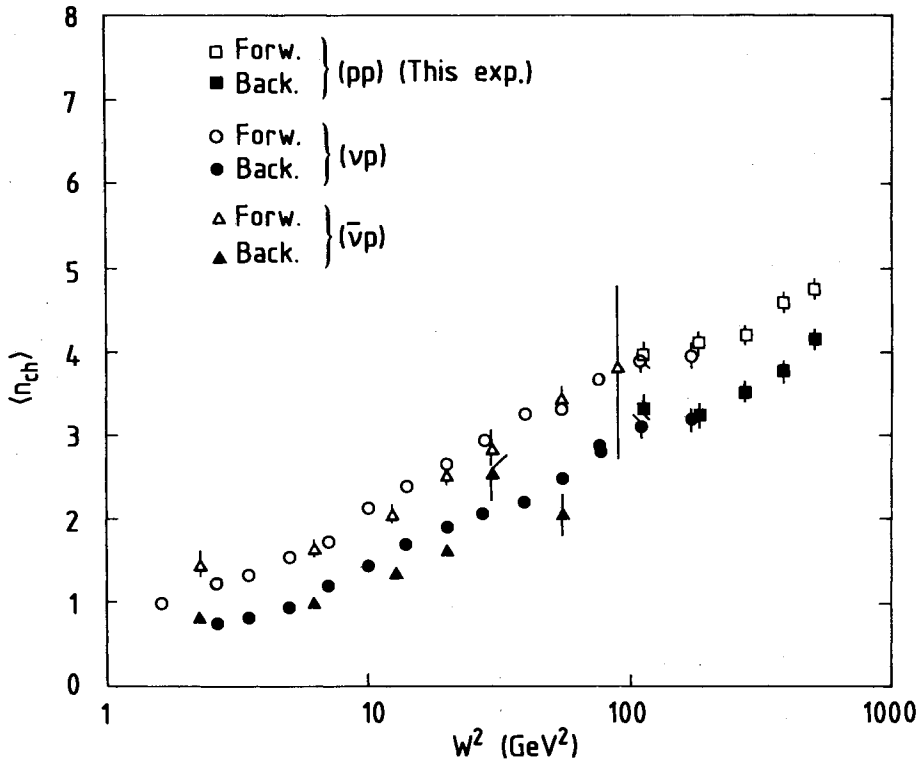

Fig. 14 The mean charged-particle multiplicities $\langle n_{ch} \rangle_{F,B}$ in the forward and backward hemispheres versus W^2, in (νp), ($\bar{\nu}$p), and (pp) interactions.

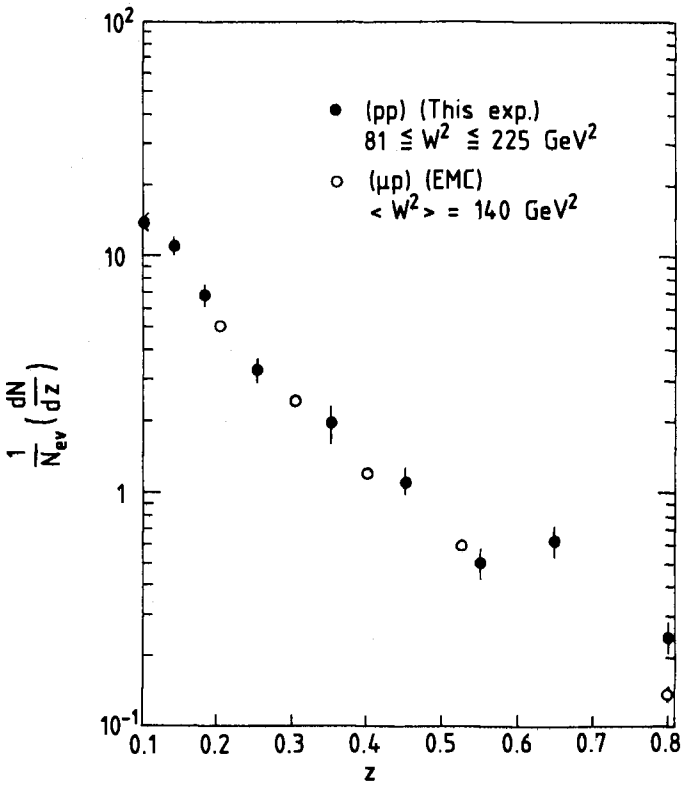

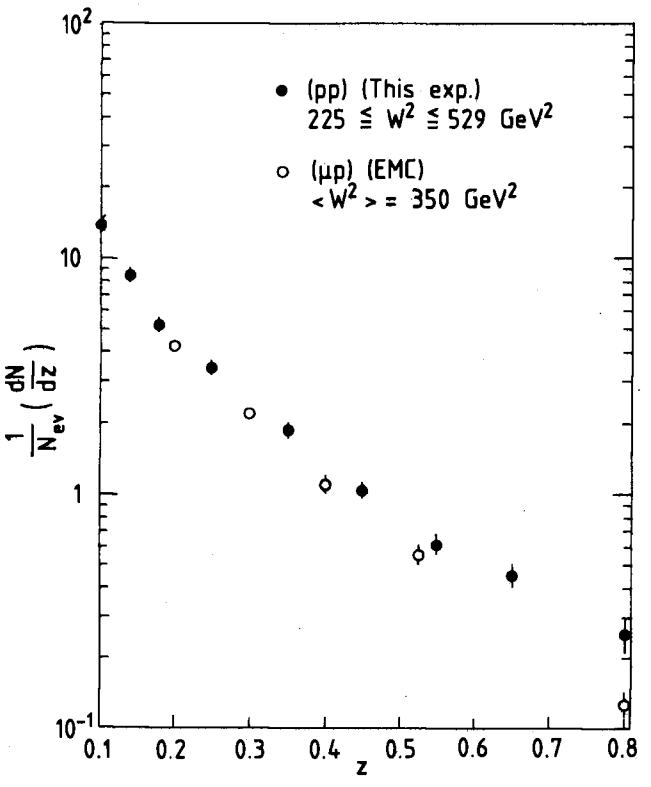

Fig. 15 The inclusive distribution of the fractional energy z for (pp) reactions: a) in the energy interval $(81 \leq W^2 \leq 225)$ GeV^2 compared with the data from (μp) reactions at $\langle W^2 \rangle$ = 140 GeV ; b) in the energy interval $(225 \leq W^2 \leq 529)$ GeV^2, compared with the data from (μp) reactions at $\langle W^2 \rangle$ = 350 GeV^2.